

## Data Analysis of Motorcycle in a Motard Race

A.Shinagawa<sup>\*</sup>, H.Nozawa<sup>#</sup>, T.Masuda<sup>†</sup>

<sup>\*</sup> Yamaha Motor, Co., Ltd.

2500 Shingai, Iwata, Shizuoka, 438-8501, Japan  
e-mail: shinagawaa@yamaha-motor.co.jp

<sup>#</sup> Yamaha Motor, Co., Ltd.

2500 Shingai, Iwata, Shizuoka, 438-8501, Japan  
e-mail: nozawahis@yamaha-motor.co.jp

<sup>†</sup> JAWS, Co., Ltd.

164-2 Takamachi, Naka-ku, Hamamatsu, Shizuoka, 432-8015, Japan  
e-mail: jawsdnf@icloud.com

### ABSTRACT

It is thought that the first step to understanding vehicle movement is to measure and analyze that movement in order to confirm that it falls within the range of the laws of physics. In the case of a four-wheeled vehicle, in general, the friction limit is defined within the circle of longitudinal acceleration and lateral acceleration through the use of a G-G diagram. Then measurements are taken to confirm that the driving state is within that range. An investigation was conducted to confirm if this G-G diagram could be applied to a two-wheeled vehicle. Measurements were taken during actual motard racing by top-class Japanese motard motorcycle riders. As a result, it was confirmed that shape and size of the analyzed G-G diagram generally matched up with the assumed friction circle. Consequently, it was confirmed that it is possible to use a G-G diagram to accurately grasp the vehicle movement limits and the associated driving state for two-wheeled vehicles.

**Keywords:** Motorcycle, G-G Diagram, Acceleration, Asphalt Road, Dirt Road, Measurement

### 1 INTRODUCTION

It is thought that the first step to understanding vehicle movement is to measure and analyze that movement in order to confirm that it falls within the range of the laws of physics. In the case of a four-wheeled vehicle, in general, the friction limit is defined within the circle of longitudinal acceleration and lateral acceleration through the use of a G-G diagram. Then measurements are taken to confirm that the driving state is within that range [1]. In the case of motorcycles, there are a few examples of these kinds of measurements and analysis. These include fundamental consideration of the turning limits [2] and creating an index for driving skill levels [3] for motorcycles driven on an asphalt road surface, as well as analyzing vehicle behavior during jumps [4] and analyzing vehicle behavior during actual races [5][6] for motorcycles driven on dirt track surfaces. However, there are no reported examples of measurement data, analysis, and a G-G diagram being applied to motorcycles. Consequently, motard (Supermoto) motorcycles that can be driven on both asphalt track surfaces and dirt track surfaces were used and measurement data was recorded during actual race riding by top-class Japanese motard motorcycle riders. The applicability of the G-G diagram to motorcycles was then verified by determining whether or not the shape and size of the analyzed G-G diagram matched the assumed friction circle.

### 2 OUTLINE OF THE MOTARD RACE

The All Japan Supermoto Championship race is a race in which Motard motorcycles, off-road motocross motorcycles equipped with road-racing tires, compete on a course that features both paved asphalt sections and off-road dirt sections. Fig. 1 and Fig. 2 show photographs of these different sections. Vehicle settings and tire selection in accordance with the specific course are

important factors because the ratio of asphalt road surface area to dirt road surface area varies from race to race. This type of racing is also characterized by “drifting” or causing the tires to slide sideways during cornering on the asphalt road surface sections. In this paper, measurement data was taken from a rider in the S1 Pro class and a rider in the S1 Open class competing in this race, referred to as “Rider A” and “Rider B” respectively, and then this measurement data was analyzed.



**Figure 1.** Asphalt road surface area.



**Figure 2.** Dirt road surface area.

### 3 MEASURING THE VEHICLE’S MOVEMENT LIMITS AND DRIVING STATE

Fig. 3 shows the acceleration in the longitudinal direction and in the lateral direction of the motorcycle. A G-G diagram is then used to express the movement limits of the motorcycle in those directions and the driving state, in the same way that it is used for a four-wheeled vehicle. The measuring instrument was selected based on the fact that it must be able to measure the acceleration in the longitudinal direction and the lateral direction as accurately as possible and also be able to be mounted on a motorcycle. There are two methods of obtaining the acceleration: one, measuring the acceleration itself with a gyro sensor, and two, differentiating the velocity that is obtained. In this paper the later of these two methods was selected. Fig. 4 shows how a commercially available, small-sized GPS logger was mounted on the rear fender of the motorcycle. The obtained data was the longitude,  $x$  [m], latitude,  $y$  [m], azimuth,  $\theta$  [rad], and velocity,  $v$  [m/s<sup>2</sup>]. The sampling time was set to be  $\Delta t$  [sec], so the longitudinal acceleration,  $a_x$  [m/s<sup>2</sup>], and lateral acceleration,  $a_y$  [m/s<sup>2</sup>], were calculated using the following equations.

$$a_x = \frac{\Delta v}{\Delta t}, \quad (1)$$

$$a_y = \frac{\Delta \theta}{\Delta t} v, \quad (2)$$



**Figure 3.** Direction of acceleration.



**Figure 4.** GPS logger.

The acceleration measured by a gyro sensor and the acceleration calculated by GPS data were compared. The longitudinal acceleration is indicated on figure 5 and the lateral acceleration is indicated on figure 6. Both values were identical well. It was possible to show that the acceleration measured by GPS is the validity.

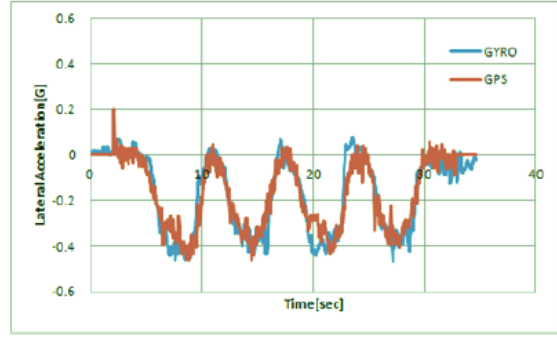
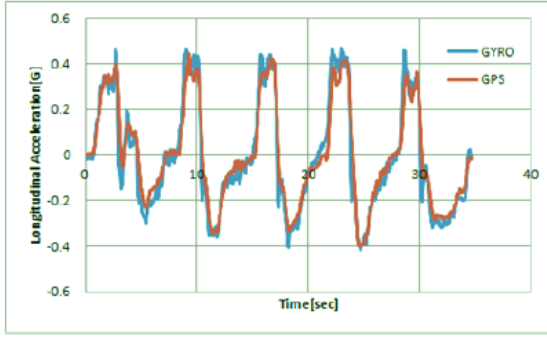


**Figure 5.** Comparison of longitudinal acceleration. **Figure 6.** Comparison of lateral acceleration.

Furthermore, the upper limit value of the acceleration, in other words, the movement limit, was expressed by the equation shown below, where the coefficient of friction of the road surface is  $\mu$  and the gravitational acceleration is  $g$  [m/s<sup>2</sup>].

$$a = \sqrt{a_x^2 + a_y^2} \leq \mu g, \quad (3)$$

In the G-G diagram this is depicted as a circle with a radius of  $\mu$ . It was assumed that the coefficient of friction of the asphalt road surface is  $\mu_A = 1.0$  and the coefficient of friction of the dirt road surface is  $\mu_D = 0.6$ . In Fig. 7, these are represented by the black circle and gray circle respectively. The applicability of the G-G diagram to motorcycles was then verified by determining whether or not the shape and size of the measured and analyzed G-G diagram matched the assumed friction circle.

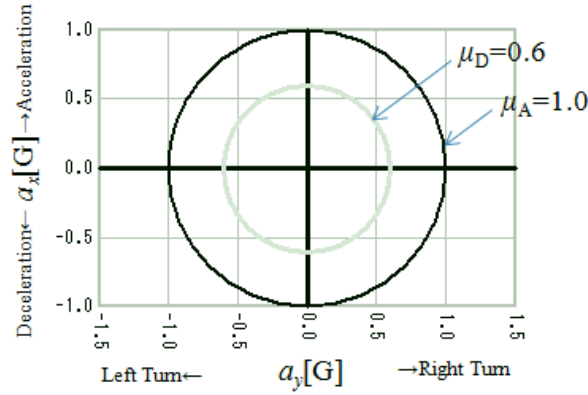


**Figure 7.** G-G diagram.

## 4 ANALYSIS OF THE RIDING DATA

### 4.1 Driving State in the Longitudinal Direction over the Whole Course

The All Japan Supermoto Championship race is held on a course that is a mixture of both paved asphalt sections and off-road dirt sections, as shown in Fig. 1 and Fig. 2. First, it is necessary to grasp the driving state for the course as a whole. Fig. 8 shows the measurement data for Rider A. This data includes the velocity,  $v$ , and the longitudinal acceleration,  $a_x$ , in a time series, as well as the running path of the motorcycle over the course. All of the graphs in this figure use color gradation to indicate the longitudinal acceleration,  $a_x$ , over a range from -1.0G to +1.0G. The data reveals that the magnitude of the longitudinal acceleration on the dirt road surface is smaller in comparison to that on the asphalt road surface. Consequently, the data from the asphalt road surface area and the dirt road surface area in Fig. 8 were extracted and the longitudi-

nal acceleration, lateral acceleration, and G-G diagrams were analyzed individually for these two areas.



**Figure 8.** Longitudinal acceleration over the whole course (Rider A).

#### 4.2 Driving State in Longitudinal Direction on the Asphalt Road Surface

The driving state of the rider in the longitudinal direction while driving on the asphalt road surface was analyzed. Fig. 9 shows the measurement data for Rider A. This data includes the velocity,  $v$ , and the longitudinal acceleration,  $a_x$ , in a time series, as well as the running path of the motorcycle over the asphalt road surface area. All of the graphs in this figure use color gradation to indicate the longitudinal acceleration,  $a_x$ , over a range from  $-1.0G$  to  $+1.0G$ . The motorcycle repeatedly performed acceleration, then deceleration, and then turning during its run on the asphalt road surface, and throughout this run the longitudinal acceleration,  $a_x$ , stayed approximately within the range of  $\pm 1.0G$ . In addition, the display of the color gradation on the running path makes it possible to confirm the driving state of the rider, such as where they are accelerating and decelerating, to what degree are they accelerating and decelerating, and whether or not this is linked to their lateral movement. Fig. 10 shows the driving state of Rider B on the same asphalt road surface area for comparison. The data indicates that the driving state of Rider A includes larger accelerations and decelerations. This is expressed in the color gradation by the darker shades of red and blue.

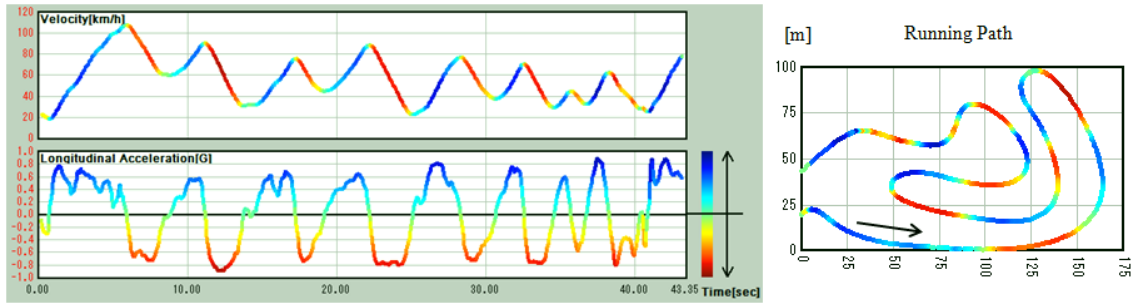


**Figure 9.** Longitudinal acceleration on asphalt road surface area (Rider A).

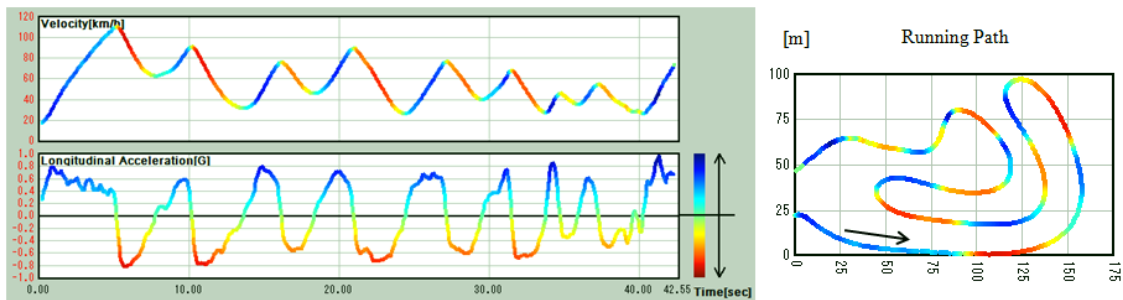


**Figure 10.** Longitudinal acceleration on asphalt road surface area (Rider B).

### 4.3 Driving State in Lateral Direction on the Asphalt Road Surface

The driving state of the rider in the lateral direction while driving on the asphalt road surface was analyzed. Fig. 11 shows the measurement data for Rider A. This data includes the velocity,  $v$ , and the lateral acceleration,  $a_y$ , in a time series, as well as the running path of the motorcycle over the asphalt road surface area. All of the graphs in this figure use color gradation to indicate the lateral acceleration,  $|a_y|$ , over a range from 0 to 1.2G. The lateral acceleration,  $a_y$ , during the run on the asphalt road surface area was slightly more than approximately  $\pm 1.0G$ . Fig. 12 shows the driving state of Rider B on the same asphalt road surface area for comparison. In the case of the driving state for Rider B, the turning velocity was generally higher than that of Rider A. Consequently, the color gradation in the corners shows a darker shade of red.

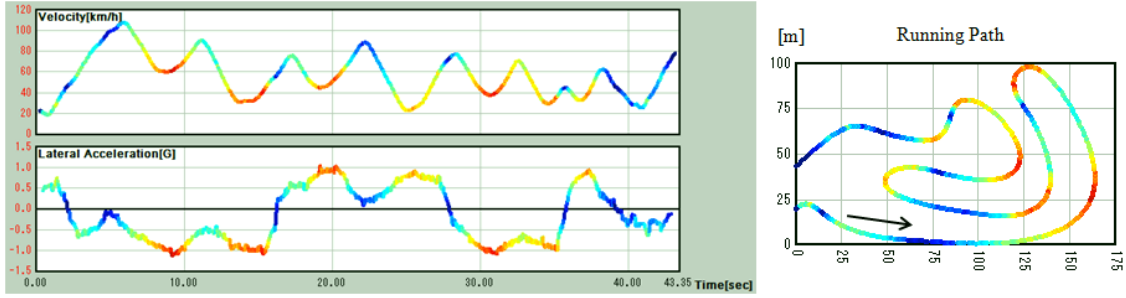


Figure 11. Lateral acceleration on asphalt road surface area (Rider A).

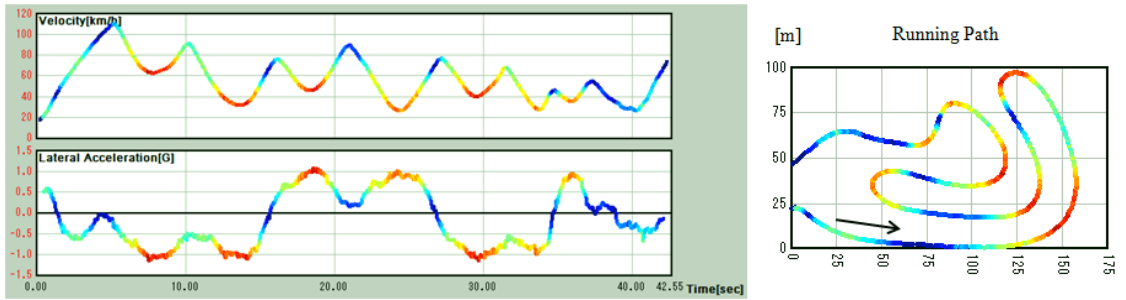
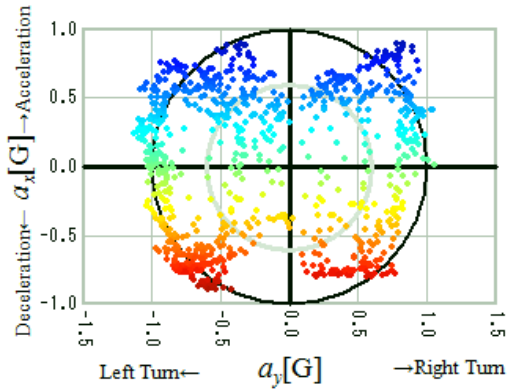


Figure 12. Lateral acceleration on asphalt road surface area (Rider B).

### 4.4 Driving State in Longitudinal and Lateral Directions on the Asphalt Road Surface

The driving state of the rider in the longitudinal and lateral directions while driving on the asphalt road surface was analyzed. Fig. 13 shows measurement data for Rider A in the form of a G-G diagram where the lateral acceleration is on the horizontal axis and the longitudinal acceleration is on the vertical axis. This figure uses a color gradation to indicate the longitudinal acceleration,  $a_x$ , over a range from -1.0G to +1.0G. The data shows that there are few acceleration and deceleration actions performed with the rider is in a fully upright state, so the driving state is one in which deceleration and turning, as well as turning and acceleration are often occurring at the same time. The black circle in Fig. 11 represents where  $\mu_A = 1.0$ , but the measurement data slightly exceeded this circle in the horizontal direction. Fig. 14 shows the driving state of Rider B for comparison. The data in these two figures indicates that the riding style of Rider A produced large longitudinal acceleration, while the riding style of Rider B produced large lateral acceleration. This data also indicates that the shape and size of the analyzed G-G diagram generally matched the assumed friction circle at  $\mu_A = 1.0$ . Consequently, it was confirmed that it is appropriate to apply the G-G diagram on the asphalt road surface to motorcycles.



**Fig 13.** G-G Diagram for asphalt road surface area (Rider A).

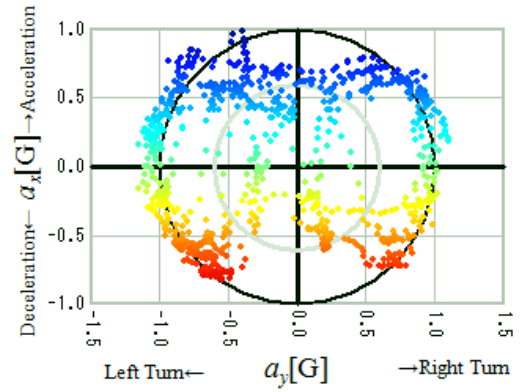


**Fig 14.** G-G Diagram for asphalt road surface area (Rider B).

#### 4.5 Driving State in Longitudinal Direction on the Dirt Road Surface

The driving state of the rider in the longitudinal direction while driving on the dirt road surface was analyzed. Fig. 15 shows the measurement data for Rider A. This data includes the velocity,  $v$ , and the longitudinal acceleration,  $a_x$ , in a time series, as well as the running path of the motorcycle over the dirt road surface area. All of the graphs in this figure use color gradation to indicate the longitudinal acceleration,  $a_x$ , over a range from -1.0G to +1.0G. During the run, the longitudinal acceleration,  $a_x$ , stayed generally within a range of about  $\pm 0.6G$ . In the areas of the graphs where the value exceeds 0.6G, it has been surmised that these are corners where the dirt road surface has been given a camber and so the values here exceed the coefficient of friction due to the shape effect. Fig. 16 shows the driving state of Rider B for comparison. The data indicates that the driving state of Rider A includes a higher motorcycle velocity and larger accelerations and decelerations. This is expressed in the color gradation by the darker shades of red and blue.

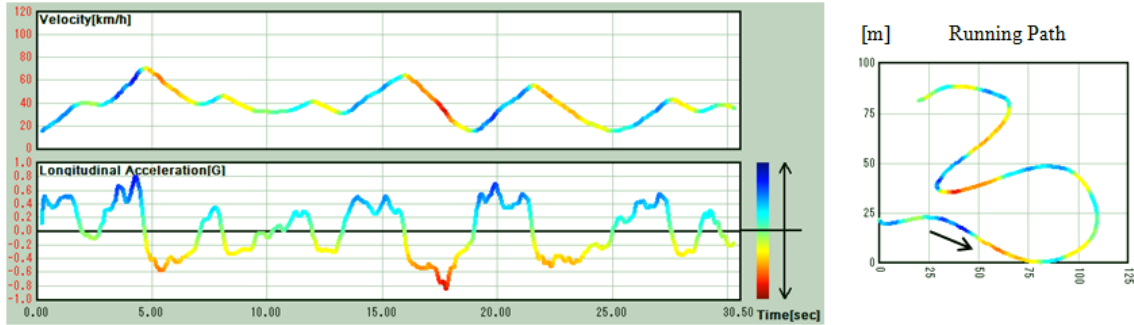


**Figure 15.** Longitudinal acceleration on dirt road surface area (Rider A).

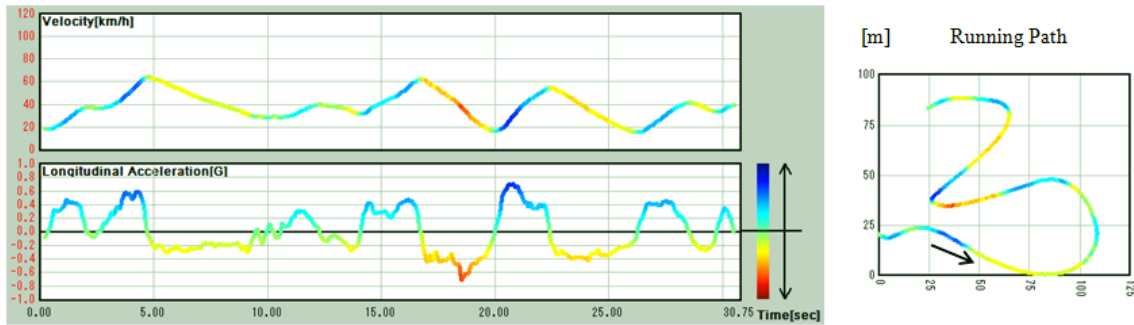


**Figure 16.** Longitudinal acceleration on dirt road surface area (Rider B).



#### 4.6 Driving State in Lateral Direction on the Dirt Road Surface

The driving state of the rider in the lateral direction while driving on the dirt road surface was analyzed. Fig. 17 shows the measurement data for Rider A. This data includes the velocity,  $v$ , and the lateral acceleration,  $a_y$ , in a time series, as well as the running path of the motorcycle over the dirt road surface area. All of the graphs in this figure use color gradation to indicate the lateral acceleration,  $|a_y|$ , over a range from 0 to 1.2G. The lateral acceleration,  $a_y$ , during the run on the dirt road surface area was approximately within a range of  $\pm 0.6G$ . In the areas of the graphs where the value exceeds 0.6G, it has been surmised that the values here exceed the coefficient of friction due to the influence of the banked dirt road surface, the same as in the case of the acceleration in the longitudinal direction. The time series data for the lateral acceleration is unstable in the area where a large turning radius is drawn. This illustrates how it is more difficult to keep the lateral acceleration constant on a flat dirt road than on the asphalt road surface. Fig. 18 shows the driving state of Rider B for comparison. The data indicates that Rider A is able to perform steady turns at a higher motorcycle velocity.

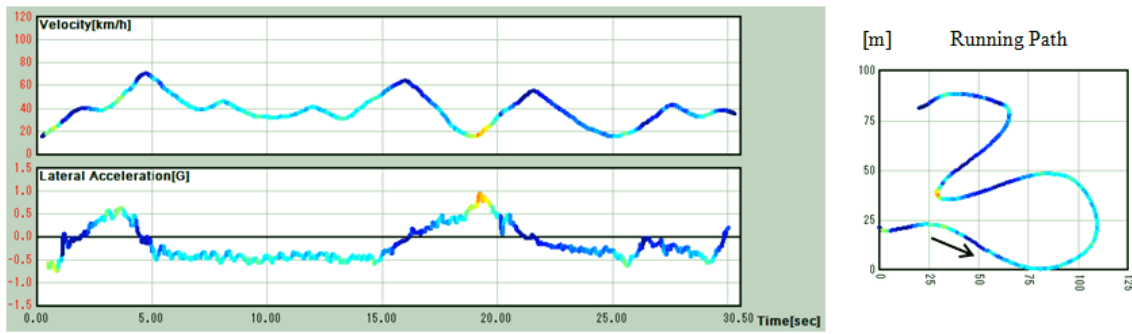


Figure 17. Lateral acceleration on dirt road surface area (Rider A).

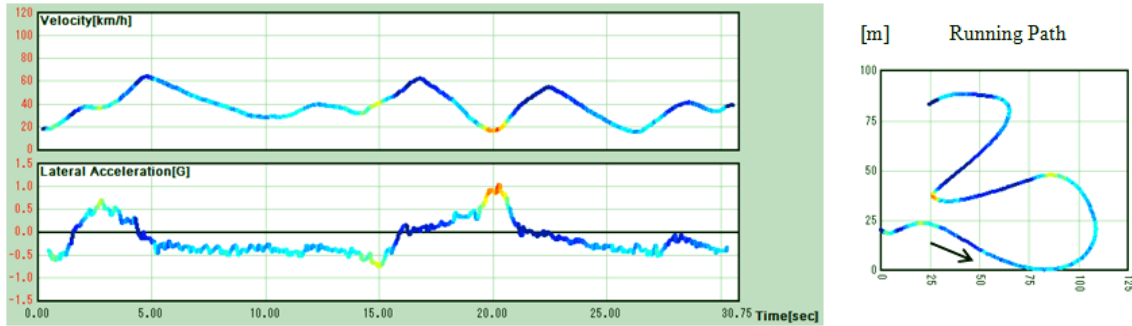
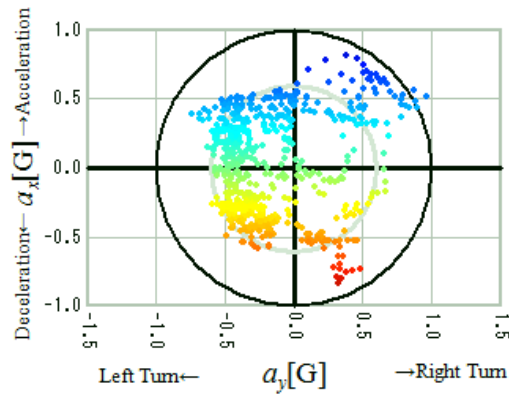


Figure 18. Lateral acceleration on dirt road surface area (Rider B).

#### 4.7 Driving State in Longitudinal and Lateral Directions on the Dirt Road Surface

The driving state of the rider in both the longitudinal and lateral directions while driving on the dirt road surface was analyzed. Fig. 19 shows measurement data for Rider A in the form of a G-G diagram where the lateral acceleration is on the horizontal axis and the longitudinal acceleration is on the vertical axis. This figure uses a color gradation to indicate the longitudinal acceleration,  $a_x$ . The grey circle in Fig. 19 represents where  $\mu_D = 0.6$ , but when the measurement data influenced by the camber of the dirt road surface is excluded the data values generally fall within the range of this circle. Fig. 20 shows the driving state of Rider B for comparison. The data shows that Rider A has a larger spread of the data points on their scatter diagram, so this rider was driving closer to the performance limits even under these slippery dirt road surface conditions. This data also indicates that the shape and size of the analyzed G-G diagram generally matched the assumed friction circle at  $\mu_D = 0.6$ . Consequently, it was confirmed that it is appropriate to apply the G-G diagram on the dirt road surface to motorcycles.



**Figure 19.** G-G Diagram for dirt road surface area (Rider A).

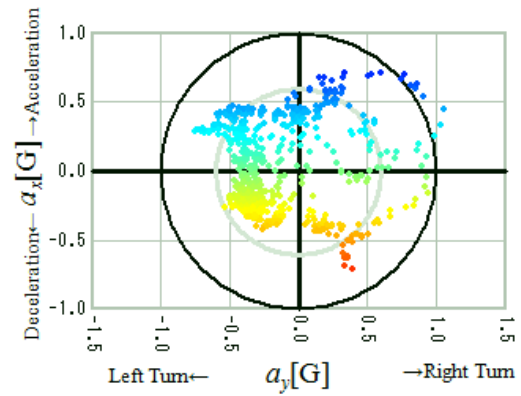


**Figure 20.** G-G Diagram for dirt road surface area (Rider B).

## 5 CONCLUSIONS

The G-G diagram is a useful tool for grasping the movement limits of a vehicle and the driving state, so its applicability to motorcycles was examined. To this end, Motard motorcycles that can be driven on both asphalt and dirt road surfaces were used and measurement data was taken from top-class riders during the All Japan Supermoto Championship race. As a result, it was confirmed that the shape and size of the analyzed G-G diagram generally matched up with the assumed friction circles for the asphalt road surface and dirt road surface respectively. Consequently, it was shown that it is possible to use a G-G diagram to grasp the movement limits of motorcycles and the driving state.

## REFERENCES

- [1] D. Umetsu, T. Okamoto, A. Yagi, Y. Mushitani, et al., “Development of Harmonized Dynamic Feel of New Premacy” *Mazda Technical Report* 28:13-18, 2010.
- [2] H. Sakai, “Turning Limits of Motorcycles” (in Japanese) presented at the 25th Conference of the Transportation & Logistics Division of the Japan Society of Mechanical Engineers (TRANSLOG 2016) 1128, 2016.
- [3] K. Morishima, H. Daimoto, “Fundamental Study on the Quantification of the Riding Skills of Motorcycle Riders” *Yamaha Motor Company Technical Report* 48:71-80, 2012.
- [4] E. Yagi, T. Kubota, M. Sakamoto, S. Yokoyama, “Accelerating and Jumping Motion Simulations on a Motorcycle-Rider System” *Transactions of the Japan Society of Mechanical Engineers Series C* 72 (715):134-140, 2009.
- [5] Y. Nakamura, “Data Measurement during an All Japan Motocross Race” (in Japanese) *Motor Ring* 30, 2010.
- [6] A. Shinagawa, H. Nozawa, Y. Uchiyama, “Data Analysis of Off-Road Motorcycle in Japan National Cross-Country” presented at the 25th Conference of the Transportation & Logistics Division of the Japan Society of Mechanical Engineers (TRANSLOG 2016) 1126, 2016.